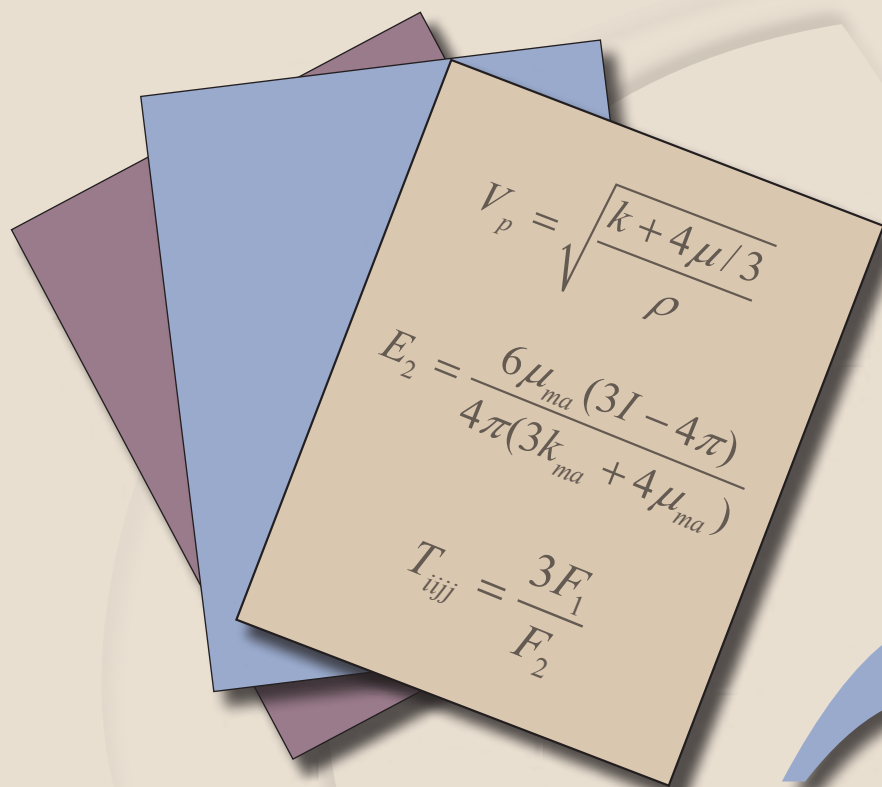![USGS logo](science for a changing world)

Comparison of the Modified Biot-Gassmann Theory and the Kuster-Toksöz Theory in Predicting Elastic Velocities of Sediments

$$V_p = \sqrt{\frac{k + 4\mu/3}{\rho}}$$

$$E_2 = \frac{6\mu_{ma}(3I - 4\pi)}{4\pi(3k_{ma} + 4\mu_{ma})}$$
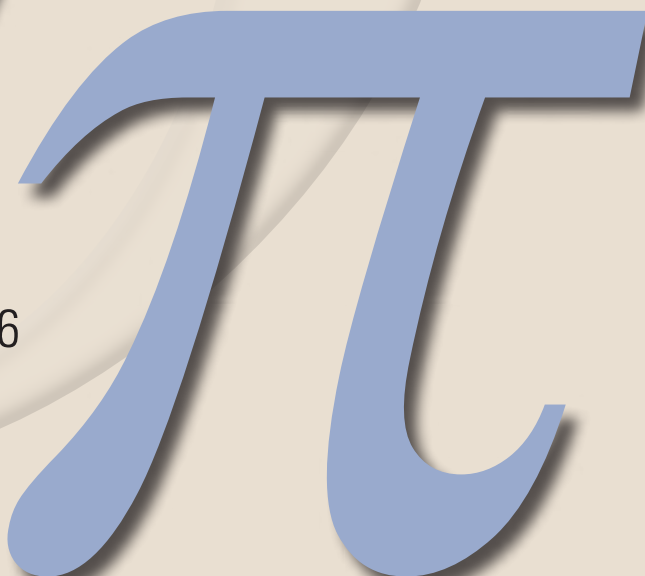
$$T_{iijj} = \frac{3F_1}{F_2}$$

Scientific Investigations Report 2008–5196

Comparison of the Modified Biot-Gassmann Theory and the Kuster-Toksöz Theory in Predicting Elastic Velocities of Sediments

By Myung W. Lee

U.S. Department of the Interior
DIRK KEMPTHORNE, Secretary

U.S. Geological Survey
Mark D. Myers, Director

U.S. Geological Survey, Reston, Virginia: 2008

Contents

Figures

Table

Abbreviations Used in This Report

BGT	Biot-Gassmann theory
BGTL	modified Biot-Gassmann theory of Lee
KTT	Kuster-Toksöz theory
KTT–GM	Kuster-Toksöz theory–Gassmann theory
GPa	gigapascal (10^9 pascal)
km/s	kilometer per second
MPa	megapascal

Conversion Factors

Multiply	By	To obtain
GPa	9,869	atmosphere
km/s	0.621	mile per second
MPa	9.869	atmosphere

Comparison of the Modified Biot-Gassmann Theory and the Kuster-Toksöz Theory in Predicting Elastic Velocities of Sediments

By Myung W. Lee

Abstract

Elastic velocities of water-saturated sandstones depend primarily on porosity, effective pressure, and the degree of consolidation. If the dry-frame moduli are known, from either measurements or theoretical calculations, the effect of pore water on velocities can be modeled using the Gassmann theory. Kuster and Toksöz (1974, Geophysics, v. 39, p. 587–606) developed a theory based on wave-scattering theory for a variety of inclusion shapes, which provides a means for calculating dry- or wet-frame moduli. In the Kuster-Toksöz theory, elastic wave velocities through different sediments can be predicted by using different aspect ratios of the sediment's pore space. Elastic velocities increase as the pore aspect ratio increases (larger pore aspect ratio describes a more spherical pore). On the basis of the velocity ratio, which is assumed to be a function of $(1-\phi)^n$, and the Biot-Gassmann theory, Lee (2002, Geophysics, v. 67, p. 1711–1719) developed a semi-empirical equation for predicting elastic velocities, which is referred to as the modified Biot-Gassmann theory of Lee. In this formulation, the exponent n, which depends on the effective pressure and the degree of consolidation, controls elastic velocities; as n increases, elastic velocities decrease. Computationally, the role of exponent n in the modified Biot-Gassmann theory by Lee is similar to the role of pore aspect ratios in the Kuster-Toksöz theory. For consolidated sediments, either theory predicts accurate velocities. However, for unconsolidated sediments, the modified Biot-Gassmann theory by Lee performs better than the Kuster-Toksöz theory, particularly in predicting S-wave velocities.

Introduction

Numerous studies relate physical properties of rock to geophysical observations. A brief review is provided here, and a more comprehensive discussion is given by Mavko and others (1998), who brought together much of the theory and the data forming the foundation of rock physics.

Biot (1956) developed theoretical formulas for predicting the frequency-dependent elastic velocities of water-saturated rocks in all frequency ranges, and Geertsma and Smit (1961) analyzed the Biot equation for dilatational waves in the low-frequency range.

Gassmann (1951) derived equations for elastic velocities of the fluid-saturated porous media at zero frequency. The Gassmann (1951) theory predicts the bulk modulus of the fluid-saturated porous medium from the known bulk moduli of the frame and the pore fluid, and it assumes that the sediment shear modulus is not affected by fluid saturation. The essential input for the application of the Gassmann equation is the bulk modulus of the dry frame, which is generally measured in the laboratory. These theories are generally applied to consolidated sediments at high effective pressure, and some empirical formulas also have been developed (for example, Wyllie and others, 1956; Raymer and others, 1980; Castagna and others, 1985; Han and others, 1986).

Moduli of dry sediments or water-saturated sediments can be calculated from the Kuster and Toksöz (1974) theory (KTT), which is based on wave scattering theory. On the basis of KTT and differential effective medium theory, Xu and White (1996) proposed a method of calculating elastic velocities using pore aspect ratios to characterize the compliance of sand and clay components. In KTT, as the pore aspect ratio increases, elastic velocities increase, so that the effect on velocities of effective pressure and the degree of consolidation can be modeled using various pore aspect ratios. Because elastic velocities depend on pore aspect ratios, KTT can be used for both consolidated and unconsolidated sediments. Also, KTT predicts that shear modulus varies with fluid saturation, which differs from the prediction of the Biot-Gassmann theory (BGT) (Thomsen, 1985).

Theories for velocities of unconsolidated sediments have been introduced: for example, the effective medium theory by Helgerud and others (1999) and Jakobsen and others (2000), and the modified Biot-Gassmann theory of Lee (herein referred to as BGTL) by Lee (2002, 2003). In BGTL, the shear modulus of water-saturated sediments is derived under the assumption that S-wave velocity (V_s) is related to the P-wave velocity (V_p) by $G(1-\phi)^n$, where G is a scalar and ϕ is porosity. Parameter n is introduced to incorporate the effect of effective pressure and the degree of consolidation on elastic velocities, and parameter G is introduced to compensate for the discrepancy between the observed V_p/V_s ratio of sediment and V_p/V_s ratio of the grains. In BGTL, as n increases, elastic velocities decrease; the effect on velocities of effective pressure and degree of consolidation is modeled using various values of n.

Because the pore aspect ratios in KTT and the exponent n in BGTL have a similar effect on predicted velocity, the performance of KTT and BGTL is compared in this paper with a variety of measured velocities for consolidated sandstones and unconsolidated sands and with well log velocities at the Alpine–1 well, North Slope of Alaska.

Theory

Modified Biot-Gassmann Theory

Lee (2003) derived a sediment shear modulus based on the assumption that $V_s = V_p G \alpha (1-\phi)^n$, where α is the V_s/V_p ratio of the grain and ϕ is porosity. G and n are parameters depending on effective pressure, consolidation, and clay content. The shear modulus is given by

$$\mu = \frac{\mu_{ma} k_{ma}(1-\beta)G^2(1-\phi)^{2n} + \mu_{ma}\beta^2 MG^2(1-\phi)^{2n}}{k_{ma} + 4\mu_{ma}[1 - G^2(1-\phi)^{2n}]/3}, \quad (1)$$

where

$$\frac{1}{M} = \frac{(\beta-\phi)}{k_{ma}} + \frac{\phi}{k_{fl}},$$

and k_{ma}, μ_{ma}, k_{fl}, ϕ, and β are the bulk and shear moduli of the matrix, the bulk modulus of the fluid, porosity, and the Biot coefficient, respectively.

For the sediment bulk modulus, the Biot-Gassmann theory (BGT) gives

$$k = k_{ma}(1-\beta) + \beta^2 M. \quad (2)$$

Elastic velocities in water-saturated sediments can be computed from the elastic moduli by the following:

$$V_p = \sqrt{\frac{k + 4\mu/3}{\rho}} \text{ and } V_s = \sqrt{\frac{\mu}{\rho}}, \quad (3)$$

where ρ is density of the formation given by $\rho = (1-\phi)\rho_{ma} + \phi\rho_{fl}$, and ρ_{ma} and ρ_{fl} are the matrix and pore fluid densities, respectively. Lee (2002) referred to the use of equations 1 and 2 for the computation of elastic velocities as the modified Biot-Gassmann theory by Lee.

For modeling soft rocks or unconsolidated sediments, the following Biot coefficient is used (Lee, 2002):

$$\beta = \frac{-183.05}{1 + e^{(\phi + 0.56468)/0.10817}} + 0.99494. \quad (4)$$

For modeling hard or consolidated formations, the equation by Raymer and others (1980) is used, as written in the following form by Krief and others (1990):

$$\beta = 1 - (1-\phi)^{3.8}. \quad (5)$$

According to Lee (2003), the exponent n is given by

$$n = [10^{(0.426 - 0.235 Log_{10}p)}]/m \quad (6a)$$

with

$$m = 1.0 + 4.95e^{5212\partial\phi/\partial p} \quad (6b)$$

and G is given by

$$G = 0.9552 + 0.0448e^{-C_v/0.06714} \quad (7)$$

where

p is effective pressure in megapascals (MPa),

m is a constant related to the degree of consolidation,

and

C_v is the clay volume in decimal units.

For a detailed discussion of parameters n and G, consult Lee (2003).

In order to accurately model the degree of consolidation in the framework of BGTL, the following geometric mean of Biot coefficient is used (Lee, 2005), which is appropriate for sediments between consolidated and unconsolidated—that is, those that are semiconsolidated or loosely consolidated as mentioned by Blangy and others (1993):

$$\beta = \beta_1^\delta \beta_2^{1-\delta} \quad (8)$$

where

β_1 is the Biot coefficient for unconsolidated sediments (equation 4),

β_2 is the Biot coefficient for consolidated sediments (equation 5),

and

δ is a weight.

The mean Biot coefficient is just the Biot coefficient for unconsolidated sediments when $\delta = 1$, and is the Biot coefficient for consolidated sediments when $\delta = 0$.

Kuster-Toksöz Theory

The Kuster-Toksöz theory (Kuster and Toksöz, 1974) is based on the long wavelength, first-order scattering phenomena of elastic waves in a two-phase medium. The medium is assumed to consist of matrix and inclusions. The effective elastic moduli of a two-phase medium that contains ellipsoidal inclusions can be written as follows:

$$k_d - k_{ma} = \frac{1}{3}(k^* - k_{ma})\frac{3k_d + 4\mu_{ma}}{3k_{ma} + 4\mu_{ma}}\sum_{l=s,c}\phi_l T_{iijj}(\alpha_l) \quad (9)$$

and

$$\mu_d - \mu_{ma} = \frac{6\mu_d(\mu^* - \mu_{ma})(k_{ma} + 2\mu_{ma}) + \mu_{ma}(9k_{ma} + 8\mu_{ma})}{5\mu_{ma}(3k_{ma} + 4\mu_{ma})}$$

$$\sum_{l=s,c}\phi_l\left[T_{ijij}(\alpha_l) - \frac{T_{iijj}(\alpha_l)}{3}\right]. \quad (10)$$

In equations 9 and 10, k_d, k_{ma}, and k^* are the bulk moduli of the dry frame, the grain, and the pore inclusion material, respectively; μ_d, μ_{ma}, and μ^* are the shear moduli of the dry frame, the grain, and the pore inclusion material, respectively. Porosity (ϕ) is assumed to consist of

stiff pores (ϕ_s) with a pore aspect ratio α_s in sandstone and compliant or soft pores (ϕ_c) with a pore aspect ratio α_c in shale. The pore aspect ratios cannot be measured directly and their estimation relies on the best fit to log or laboratory observations (Xu and White, 1996). T_{ijkl} is a fourth-order tensor that relates the uniform strain field to the strain field within an elastic inclusion.

The pore aspect ratio functions T_{iijj} and T_{ijij} are expressed as follows:

$$T_{iijj} = \frac{3F_1}{F_2} \tag{11}$$

and

$$F \equiv T_{ijij}(\alpha) - \frac{T_{iijj}(\alpha)}{3} = \frac{2}{F_3} + \frac{1}{F_4} + \frac{F_4 F_5 + F_6 F_7 - F_8 F_9}{F_2 F_4} \tag{12}$$

where

$$F_1 = 1 + A\left[\frac{3}{2}(g + \vartheta) - R(\frac{3g}{2} + \frac{5\vartheta}{2} - \frac{4}{3})\right]$$

$$F_2 = 1 + A\left[1 + \frac{3(g + \vartheta)}{2} - \frac{R(3g + 5\vartheta)}{2}\right] + B(3 - 4R)$$
$$+ \frac{A}{2}(A + 3B)(3 - 4R\left[g + \vartheta - r(g - \vartheta + 2\vartheta^2)\right])$$

$$F_3 = 1 + A\left[R(2 - \vartheta) + \frac{(1 + \alpha^2)}{\alpha^2}g(R - 1)\right]$$

$$F_4 = 1 + A\left[3\vartheta + g - R(g - \vartheta)\right] \tag{13}$$

$$F_5 = A\left[R(g + \vartheta - 4/3) - g\right] + B\vartheta(3 - 4R)$$

$$F_6 = 1 + A\left[1 + g - R(\vartheta + g)\right] + B(1 - \vartheta)(3 - 4R)$$

$$F_7 = 2 + A\left[9\vartheta + 3g - R(5\vartheta + 3g)\right] + B\vartheta(3 - 4R)$$

$$F_8 = A\left[1 - 2R + g(R - 1)/2 + \vartheta(5R - 3)/2\right] + B(1 - \vartheta)(3 - 4R)$$

$$F_9 = A\left[g(R - 1) - R\vartheta\right] + B\vartheta(3 - 4R)$$

$$A = \frac{\mu^*}{\mu} - 1, \quad B = \frac{1}{3}\left(\frac{k^*}{k_{ma}} - \frac{\mu^*}{\mu_{ma}}\right), \quad R = \frac{3\mu_{ma}}{3k_{ma} + 4\mu_{ma}},$$

$$g = \frac{\alpha^2}{1 - \alpha^2}(3\vartheta - 2), \quad \vartheta = \frac{\alpha}{(1 - \alpha^2)^{3/2}}\left[\cos^{-1}(\alpha) - \alpha\sqrt{1 - \alpha^2}\right].$$

KTT assumes that the pores are isolated and do not interact, which leads to the restriction that the pore concentration is dilute (that is, $\phi / \alpha \ll 1$). Differential effective medium theory (Cleary and others, 1980) is used to overcome this limitation by incrementally adding the pores in small steps in such a way that the noninteraction criterion is satisfied in each step (Mavko and others, 1998; Keys and Xu, 2002). Beginning with solid rock, KTT is used to compute the effective medium that results from adding a small set of pores to the matrix. The process is repeated, using the effective medium from the previous calculation as the rock matrix for the next calculation until the total pore volume has been added to the rock.

For water-saturated sediments with ellipsoidal pore aspect ratios, KTT shown in equations 9 through 13 can be used in two ways: (1) to calculate the moduli of water-saturated sediments by using the bulk modulus of water for k^* in equation 13 (referred to as KTT in this paper), or (2) to calculate the moduli for dry rock with $k^* = 0$ in equation 13 and to use Gassmann theory for water-saturated sediments (referred to as KTT–GM). Because the inclusions are isolated with respect to wave propagation, KTT simulates the behavior of very high frequency saturated rock appropriate to ultrasonic laboratory conditions (Mavko and others, 1998). At low frequencies, KTT–GM is preferred to KTT.

One particularly useful aspect of KTT is that it predicts the S-wave velocity in sediments with differing fluid saturation, which is not consistent with the prediction of the BGT. Equations 10 and 12 indicate that the shear modulus of fluid-saturated sediments is calculated using the function F, which is related to the bulk modulus of the fluid through the constant B shown in equation 13.

Moduli of Dry Frame

In the framework of the BGT, the dry frame bulk modulus (k_d) is given by the following formula by substituting $M = 0$ in equation 2:

$$k_d = k_{ma}(1 - \beta). \tag{14a}$$

In the framework of BGTL, the following shear modulus of dry frame (μ_d) can be derived from equation 1 with $M = 0$ and $n \approx 0$ under the assumption that the velocity ratio of a dry rock is almost constant irrespective of porosity (Pickett, 1963).

$$\mu_d \approx \frac{\mu_{ma} k_{ma}(1 - \beta)G^2}{k_{ma} + 4\mu_{ma}(1 - G^2)/3}. \tag{14b}$$

In the clay-free case in which $G = 1$, equation 14b is identical to the formula derived by Krief and others (1990), which means that the velocity ratio of a dry rock is identical to that of the matrix. It is noted that when $G = 1$, the ratio of k_d / μ_d depends only on the sediment grains (that is, k_{ma} / μ_{ma}). However, when $G \neq 1.0$, the ratio of k_d / μ_d also depends on G. It is noted that even though bulk and shear moduli depend on the Biot coefficient and the Biot coefficient depends on porosity, the ratio of k_d / μ_d is independent of the Biot coefficient or porosity.

In KTT, the bulk and shear moduli of a dry frame with the aspect ratio of 1.0 are given by the following (Toksöz and others, 1976):

$$k_d^{KTT} = \frac{k_{ma}(1-\phi)}{1+3\phi k_{ma}/(4\mu_{ma})} \qquad (15a)$$

$$\mu_d^{ktt} = \frac{\mu_{ma}(1-\phi)}{1+6\phi(k_{ma}+2\mu_{ma})/(9k_{ma}+8\mu_{ma})} \qquad (15b)$$

In KTT, k_d^{KTT}/μ_d^{KTT} depends explicitly on porosity, which means that the velocity ratio of dry rock is not a constant. The effect of effective pressure on the velocity ratio can be incorporated implicitly through the pore aspect ratio.

Modeling

Modified Biot-Gassmann Theory

In the framework of BGTL, the magnitude of elastic velocities in water-saturated sediments depends primarily on the exponent n and the Biot coefficient. The exponent n depends on effective pressure and the rate of porosity reduction with respect to effective pressure. The Biot coefficient depends on porosity, the degree of consolidation, and effective pressure. As shown in equation 8, the geometric average of the end member Biot coefficient can be used for semiconsolidated or loosely consolidated sediments as described by Blangy and others (1993).

Figure 1A shows three velocity trends with respect to porosities for clean consolidated, unconsolidated, and semiconsolidated sediments. Relevant elastic constants used in all models are shown in table 1. P-wave velocities for the (1) consolidated sediment are derived from BGTL, with $n = 0.3$, $C_v = 0.0$, and $\delta = 0$ (which uses the Biot coefficient given in equation 5); (2) unconsolidated sediment are derived from BGTL, with $n = 1.4$, $C_v = 0.0$, and $\delta = 1$ (which uses the Biot coefficient given in equation 4); and (3) semiconsolidated sediment are derived from BGTL, with $n = 0.52$, $C_v = 0.0$, and $\delta = 0.5$. The three data sets can be readily compared in figure 1A.

For a given Biot coefficient, BGTL contains two adjustable parameters (n and G). As shown in figure 1A, different Biot coefficients and n are used to model velocities of three sets of sediments having differing degrees of consolidation; the velocity decreases as n increases. Equation 6 indicates that n depends on effective pressure and a constant m, which is related to the porosity change with respect to effective pressure (Lee, 2003). However, in practice the porosity change with respect to effective pressure is rarely known. Therefore, the exponent n or parameter m can be treated as a free parameter to fit the measured velocities in BGTL.

The porosity ranges shown in figure 1A should be interpreted carefully, because for porosities less than the critical porosity, the mineral grains are load bearing; for porosities greater than the critical porosity, the grains are in suspension (Nur and others, 1998). Therefore, porosities of consolidated or semiconsolidated sediments cannot be greater than the critical porosity, which is about 40 percent.

Kuster and Toksöz Theory

In KTT, the pore aspect ratio controls the velocity. For a given porosity, the velocity increases as the aspect ratio increases. Velocities modeled using KTT–GM are shown in figure 1B. For these plots, velocities are calculated for consolidated sediments with $\alpha_s = 0.3$, those for semiconsolidated sediments with $\alpha_s = 0.18$, and those for unconsolidated sediments with $\alpha_s = 0.1$. The clay content, C_v, is assumed to be zero in all cases, and if shaly sandstones are used for the modeling, the pore aspect ratio related to clay should be included.

As in figure 1A, three measured data sets are shown in figure 1B along with the calculated velocities. The predicted velocities closely follow the measured velocities. However, even though the predicted velocities obtained from KTT–GM and BGTL agree well with measured velocities, the predicted velocities from BGTL differ slightly from those predicted by KTT–GM when they are extrapolated to other porosities. For example, for consolidated sediments, BGTL with $n = 0.3$ predicts $V_p = 3.5$ km/s at $\phi = 0.3$, whereas KTT–GM predicts $V_p = 3.8$ km/s. As mentioned previously, comparisons between BGTL and KTT–GM for consolidated and semiconsolidated sediments are valid for porosities less than about 40 percent.

Discussion

Kuster and Toksöz Theory With and Without Gassmann Theory

For a given porosity, velocities are calculated with respect to the pore aspect ratio. It is shown that for a given porosity and pore aspect ratio, velocities predicted by KTT are higher than those predicted by KTT–GM (fig. 2). Model results indicate that for consolidated sediments, both KTT and KTT–GM can be used to accurately predict P-wave velocities. For example, KTT with $\alpha_s = 0.2$ predicts a P-wave velocity of 4 kilometers per second (km/s) for a sediment with $\phi = 0.2$, as does KTT–GM if $\alpha_s = 0.22$. Similar results are obtained for S-wave velocities. For an unconsolidated sediment with $\phi = 0.6$, KTT with $\alpha_s = 0.05$ predicts $V_p = 1.76$ km/s, as does KTT–GM with $\alpha_s = 0.15$. However, for S-wave velocities, KTT with $\alpha_s = 0.05$ yields $V_s = 0.24$ km/s, whereas KTT–GM

A

B

EXPLANATION

▲	Data from Han and others (1986): Consolidated
○	Data from Timur (1968): Semiconsolidated
●	Data from Hamilton (1971): Unconsolidated
—☆—	BGTL for consolidated sediments
—△—	BGTL for semiconsolidated sediments
—○—	BGTL for semiconsolidated sediments

EXPLANATION

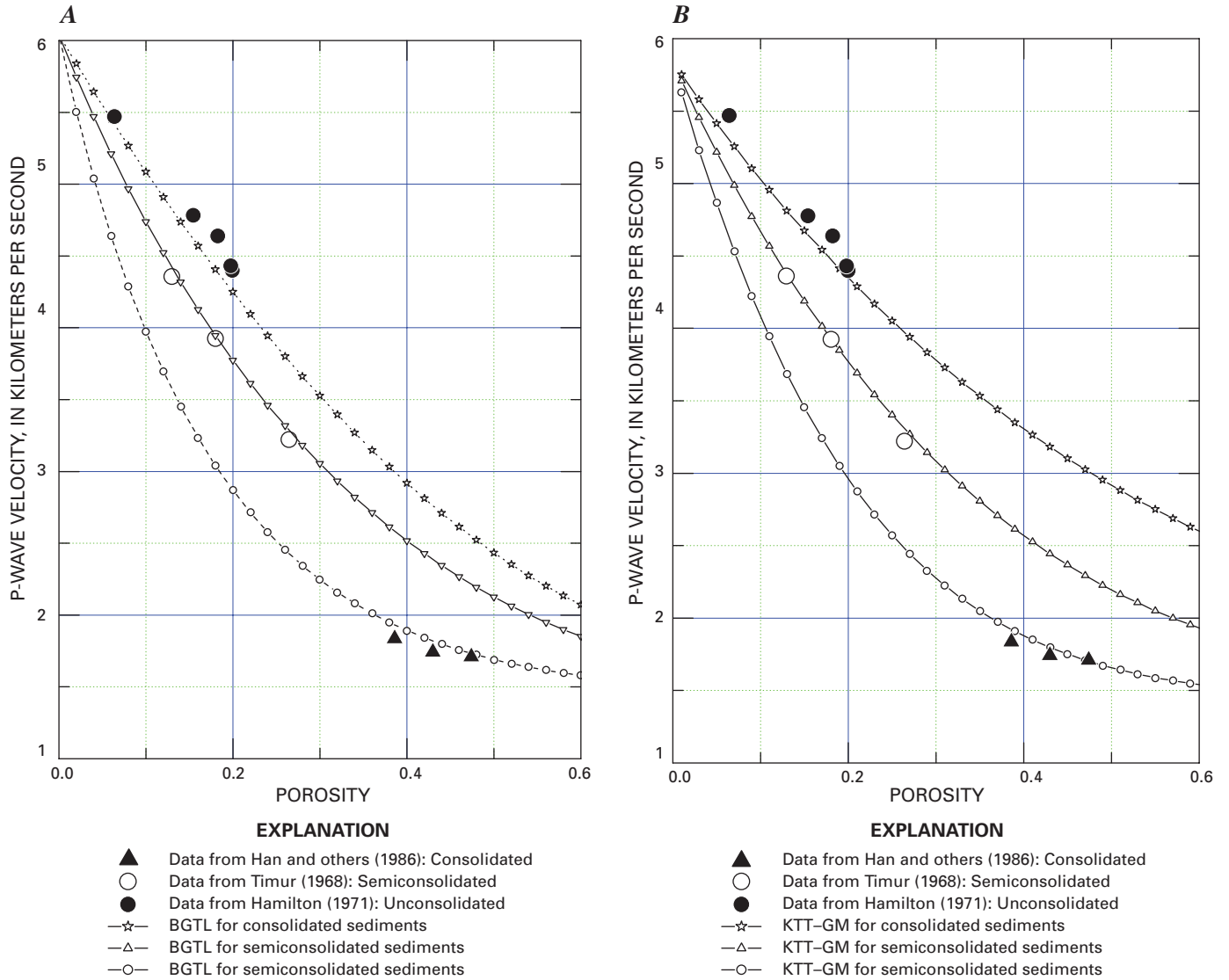|	
▲	Data from Han and others (1986): Consolidated
○	Data from Timur (1968): Semiconsolidated
●	Data from Hamilton (1971): Unconsolidated
—☆—	KTT–GM for consolidated sediments
—△—	KTT–GM for semiconsolidated sediments
—○—	KTT–GM for semiconsolidated sediments

Figure 1.   P-wave velocities predicted by the modified Biot-Gassmann theory by Lee (2002) (BGTL) and by the Kuster and Toksöz theory with Gassmann theory (KTT–GM) for unconsolidated sediments measured by Hamilton (1971), semiconsolidated sediments measured by Timur (1968), and consolidated sediments measured by Han and others (1986). *A,* Using BGTL with $n = 0.3$ and $\delta = 0$ for consolidated sediments, $n = 0.52$ and $\delta = 0.5$ for semiconsolidated sediments, and $n = 1.02$ and $\delta = 1$ for unconsolidated sediments; *B,* Using KTT with $\alpha_s = 0.3$ for consolidated sediments, $\alpha_s = 0.18$ for semiconsolidated sediments, and $\alpha_s = 0.1$ for unconsolidated sediments. ϕ, porosity.

Table 1.   Elastic constants used in velocity models.

| Parameter	Value	Source
Shear modulus of quartz	44 GPa[1]	Carmichael (1989)
Bulk modulus of quartz	38 GPa	Carmichael (1989)
Shear modulus of clay	6.85 GPa	Helgerud and others (1999)
Bulk modulus of clay	20.9 GPa	Helgerud and others (1999)
Bulk modulus of water	2.29 GPa	Lee (2002)
Density of quartz	2.65 g/cm^3	Helgerud and others (1999)
Density of clay	2.58 g/cm^3	Helgerud and others (1999)

[1]GPa, gigapascal, = 10^9 pascal
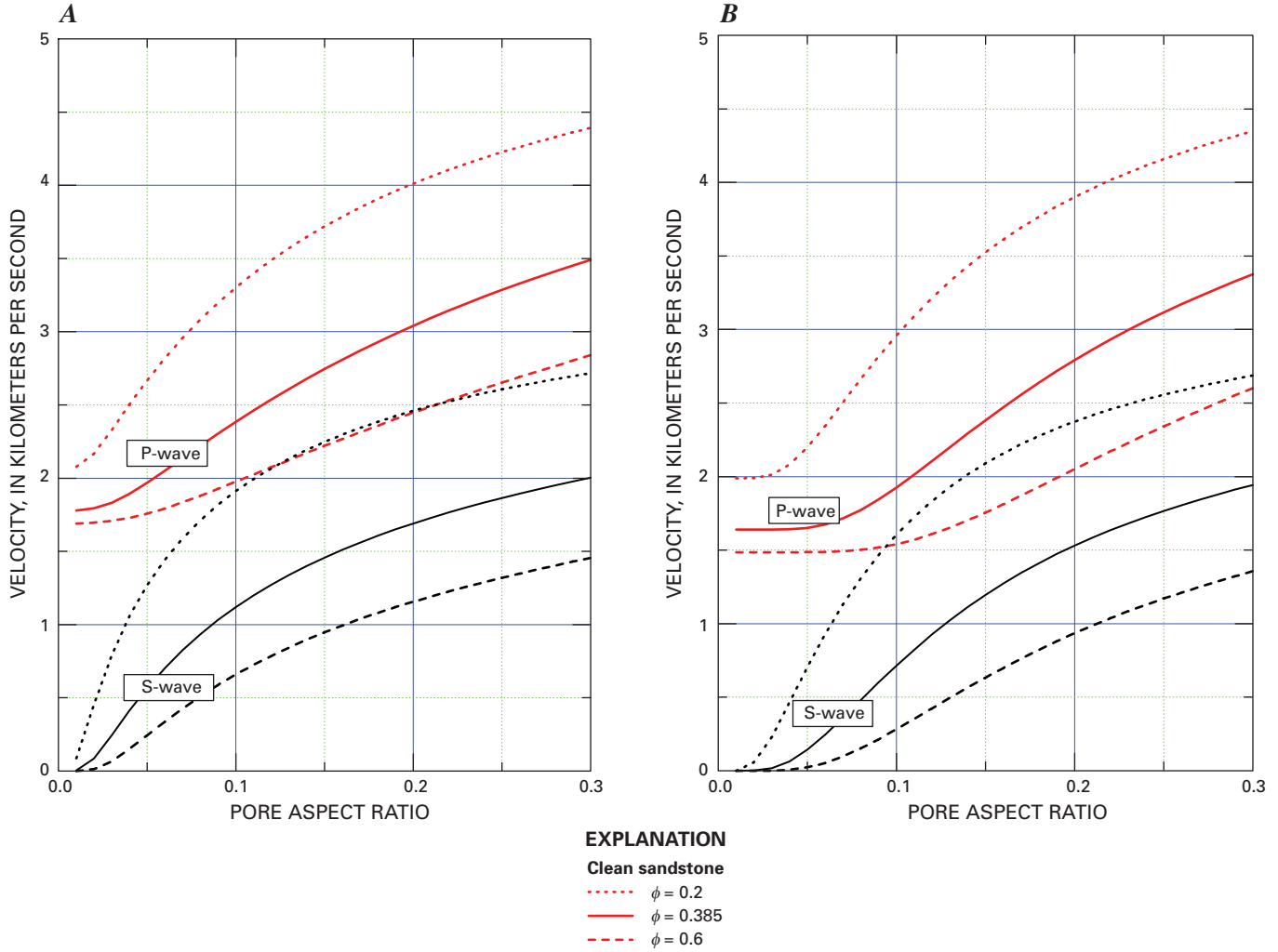
Figure 2.   Modeled P- and S-wave velocities with respect to pore aspect ratios of clean sandstones. *A*, Using Kuster and Toksöz theory (KTT); *B*, Using Kuster and Toksöz theory with Gassmann theory (KTT–GM). ϕ, porosity.

with $\alpha_s = 0.15$ yields $V_s = 0.63$ km/s. These results show that for high-porosity sediments, the S-wave prediction given by KTT is noticeably different from that given by KTT–GM.

For a high-porosity sediment ($\phi = 0.6$), the P-wave velocity predicted by KTT approaches 1.7 km/s as the pore aspect ratio approaches zero, whereas the P-wave velocity predicted by KTT–GM approaches the more realistic 1.5 km/s. This result implies that KTT is not accurate in predicting velocities for high-porosity unconsolidated sediments. Figure 3 shows an example of KTT and KTT–GM predictions for high-porosity unconsolidated marine sediments. KTT with $\alpha_s = 0.1$ and $\alpha_c = 0.03$ predicts fairly accurate S-wave velocities, but it overestimates P-wave velocities. On the other hand, KTT–GM with $\alpha_s = 0.14$ and $\alpha_c = 0.12$ predicts accurate P- and S-wave velocities. Figures 2 and 3 indicate that KTT–GM performs better than KTT in predicting elastic velocities for unconsolidated, high-porosity water-saturated sediments. Also at low frequencies, when there is time for wave-induced pore pressure increments to flow and

equilibrate, the KTT–GM approach is preferable for finding the effective moduli of dry cavities and then saturating them with Gassmann low-frequency relations (Mavko and others, 1999). Accordingly, all the results following this section are generated using KTT–GM.

Comparison of Kuster and Toksöz-Gassmann Theories and Modified Biot-Gassmann Theory of Lee

The performance of KTT–GM and BGTL for consolidated sediments differs slightly from that for unconsolidated sediments. However, the general behavior of KTT–GM and BGTL can be deduced from an analysis of velocities measured for semiconsolidated sediments.

Figure 4 shows predicted and measured velocities for Troll sandstones, which are described as loosely consolidated sediments by Blangy and others (1993). Circles and dots in figure 4*A* show velocities measured at an effective pressure
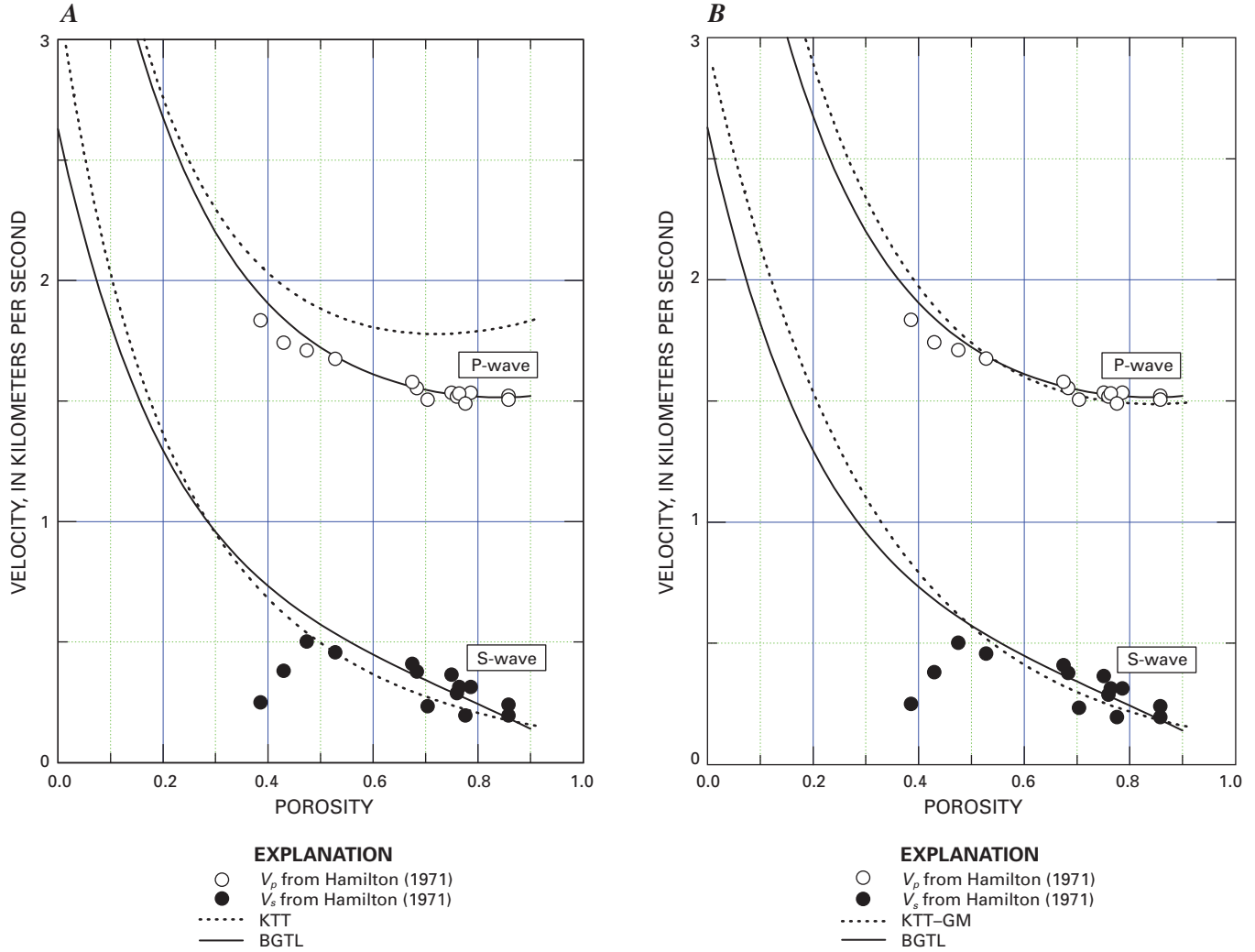
A

B

EXPLANATION

○ V_p from Hamilton (1971)
● V_s from Hamilton (1971)
......   KTT
——   BGTL

EXPLANATION

○ V_p from Hamilton (1971)
● V_s from Hamilton (1971)
......   KTT–GM
——   BGTL

Figure 3.   Modeled velocities obtained by using Kuster and Toksöz theory (KTT) and Kuster and Toksöz theory with Gassmann theory (KTT–GM), both compared with modified Biot-Gassmann theory by Lee (BGTL) with $n = 0.8$ and $C_v = 0.3$ with respect to porosity for unconsolidated sediment measured by Hamilton (1971). P-wave velocities (V_p) are measured velocities, but S-wave velocities (V_s) are computed velocities. *A*, Using KTT with $\alpha_s = 0.1$, $\alpha_c = 0.03$, and $C_v = 0.3$; *B*, Using KTT–GM with $\alpha_s = 0.14$, $\alpha_c = 0.12$, and $C_v = 0.3$. ϕ, porosity.

of 5 MPa; solid lines are predicted velocities using BGTL with $n = 1.22$, $\delta = 0.5$, and $C_v = 0.0$; and dotted lines are predicted velocities using KTT–GM with $\alpha_s = 0.13$ and $C_v = 0.0$. Predicted P-wave velocities from BGTL and KTT–GM agree well with the measured V_p. However, KTT–GM overestimates V_s, whereas V_s from BGTL agrees well with the measured V_s. Figure 4*B* shows measured and predicted velocities of Troll sandstones at the effective pressure of 30 MPa—solid lines are predicted velocities using BGTL with $n = 0.8$, $\delta = 0.5$, and $C_v = 0.0$; and dotted lines are predicted velocities using KTT–GM with $\alpha_s = 0.15$ and $C_v = 0.0$. The same conclusions can be drawn from model results regarding measured and predicted velocities at both effective pressures.

Because velocities depend on effective pressure, the parameter n in BGTL changes from $n = 1.22$ at 5 MPa to $n = 0.8$ at 30 MPa, whereas the parameter α_s in KTT–GM

changes from $\alpha_s = 0.13$ at 5 MPa to $\alpha_s = 0.15$ at 30 MPa. Figure 4 also indicates that the predicted V_s from KTT–GM is generally greater than the measured V_s, but the difference decreases as effective pressure increases.

Figures 5 and 6 show velocities of consolidated sediments measured by Han and others (1986). Figure 5 is a plot of velocities predicted from porosity and clay volume content by using KTT–GM. For data at 5 MPa (fig. 5*A*), the values of $\alpha_s = 0.2$ and $\alpha_c = 0.1$ are used. Fractional errors for the predicted V_p are 0.00 ± 0.04 and 0.07 ± 0.08 for V_s, indicating that KTT–GM predicts P-wave velocities more accurately than S-wave velocities. However, the inaccuracy in the S-wave velocity results from adjusting the pore aspect ratios to fit the P-wave velocities. For 40 MPa data (fig. 5*B*), $\alpha_s = 0.3$ and $\alpha_c = 0.15$ are used for KTT–GM. The fractional errors are 0.01 ± 0.04 and 0.04 ± 0.05 for the predicted P-wave and S-wave velocities,
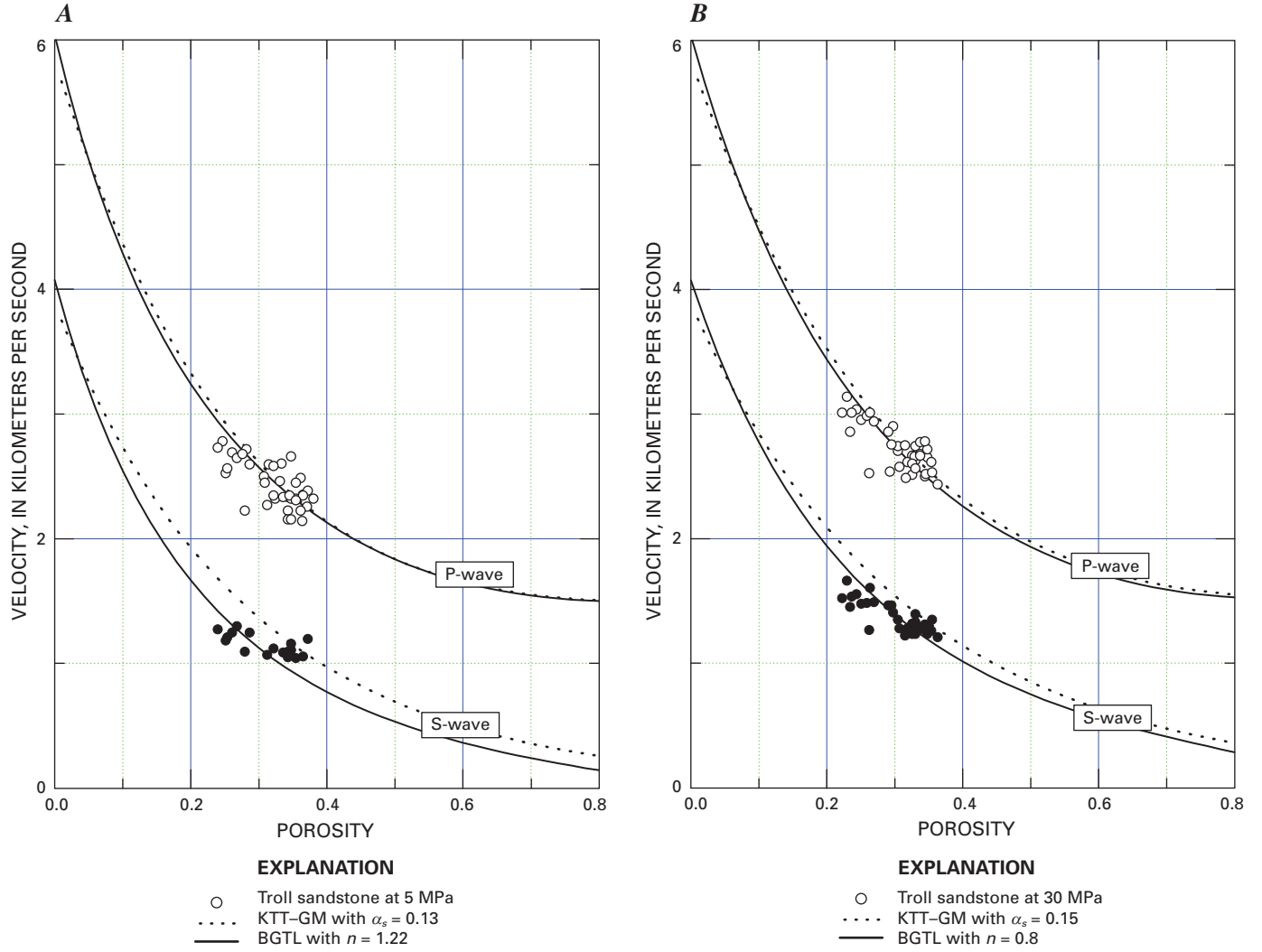
Figure 4.   Measured P- and S-wave velocities compared with predicted velocities obtained by using the modified Biot-Gassmann theory by Lee (2002) (BGTL) and the Kuster and Toksöz theory with Gassmann theory (KTT–GM) for semiconsolidated, clay-free Troll sandstones measured by Blangy and others (1993) with respect to porosity. *A*, Velocities measured at 5 megapascals (MPa) effective pressure compared with predicted velocities using BGTL with n = 1.22 and KTT–GM with α_s = 0.13; *B*, Velocities measured at 30 MPa effective pressure compared with predicted velocities using BGTL with n = 0.8 and KTT–GM with α_s = 0.15. ϕ, porosity.

respectively. The accuracies of P-wave velocities are similar, but the accuracy of S-wave velocities increases as effective pressure increases.

Figure 6 shows the same results by using BGTL with n = 0.73 for 5 MPa data and n = 0.2 for 40 MPa data with the Biot coefficient for consolidated sediments (δ = 0). The fractional error for P-wave velocity at 5 MPa is 0.00 ± 0.04 and for V_s is –0.02 ± 0.08. The fractional errors at 40 MPa are –0.01 ± 0.02 and –0.01 ± 0.05 for P- and S-wave velocities, respectively. For all modeling, parameters are derived from the P-wave velocities and the same parameters are applied to S-wave velocities. As shown in figures 5 and 6, the fractional error for S-wave velocities predicted from KTT–GM depends on effective pressure, and it decreases as effective pressure increases. However, for BGTL, the fractional error is less

sensitive to effective pressure. Although overall errors from BGTL and KTT–GM are small, figures 5 and 6 indicate that BGTL performs somewhat better than KTT–GM in predict-ing velocities from the porosity for consolidated sediments measured by Han and others (1986).

Predicting S-Wave Velocity

One important application of BGTL or KTT–GM is the prediction of S-wave velocities for a given set of P-wave velocities and porosities. Model results indicate that KTT–GM slightly overestimates the S-wave velocities. The discrep-ancy between predicted and measured S-wave velocities increases as both the effective pressure and the degree of consolidation decrease. Figure 7 shows well log velocities at
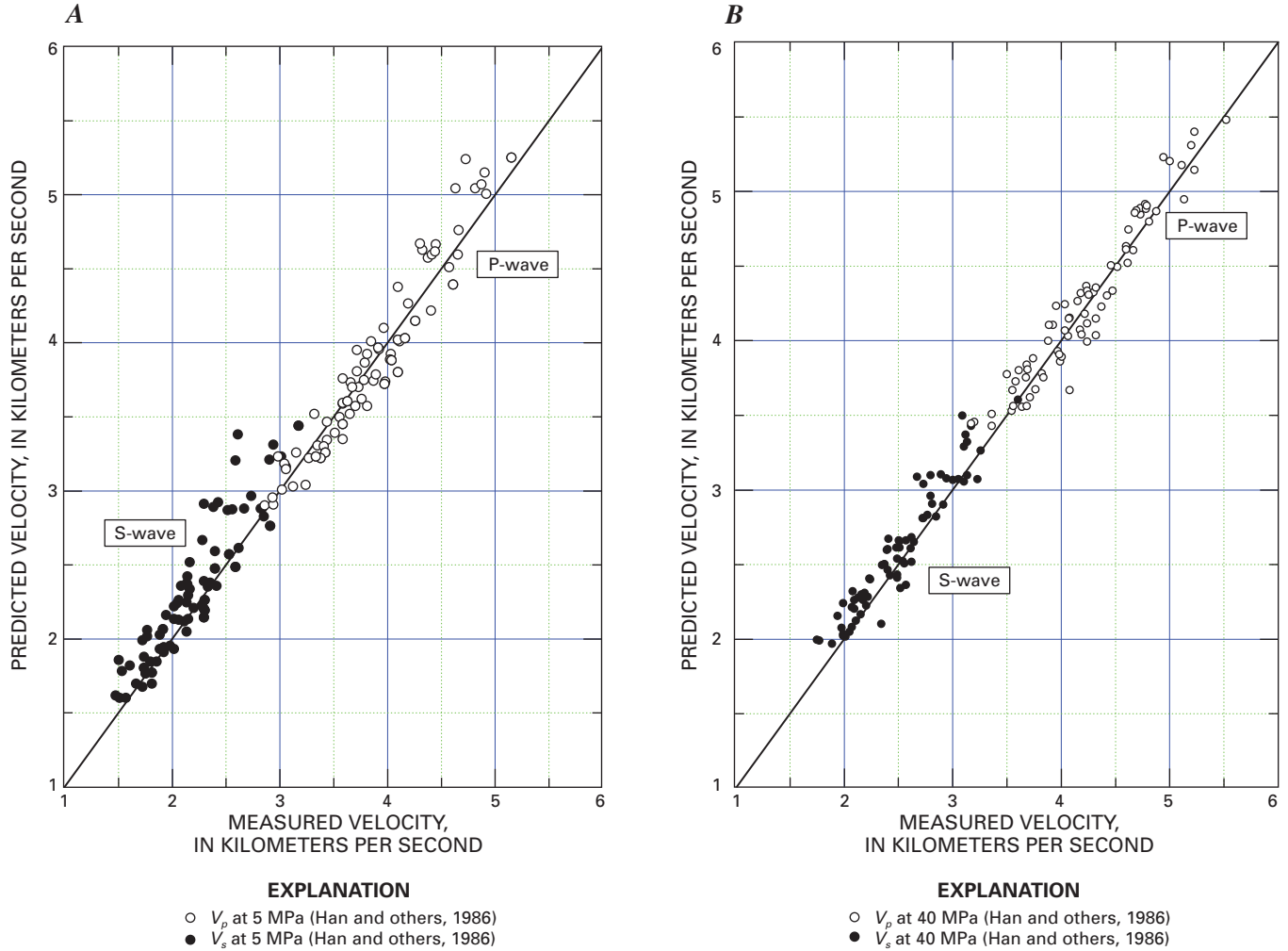
A

B

Figure 5. Measured P- and S-wave velocities (V_p, V_s) compared with predicted velocities obtained by using Kuster and Toksöz theory with Gassmann theory (KTT–GM) for consolidated sandstones measured by Han and others (1986). *A*, Velocities measured at 5 megapascals (MPa) effective pressure compared with predicted velocities using $\alpha_s = 0.2$ and $\alpha_c = 0.1$; *B*, Velocities measured at 40 MPa effective pressure compared with predicted velocities using $\alpha_s = 0.3$ and $\alpha_c = 0.15$.

the Alpine–1 well, North Slope of Alaska. The parameters for KTT–GM are $\alpha_s = 0.09$, $\alpha_c = 0.045$, and $C_v = 0.07$, which are derived from the P-wave velocities. Predicted P-wave velocities using KTT–GM with these parameters are shown as the solid line in figure 7 and agree well with the measured velocities. However, KTT–GM overestimates the S-wave velocities. On the other hand, the velocities predicted from BGTL with $n = 1.75$ and $C_v = 0.07$, shown as dotted lines, agree well with measured velocities.

Figure 8 shows the predicted S-wave velocities with respect to depth using P-wave velocities and porosities at the Alpine–1 well. Predicted S-wave velocity from KTT–GM with the pore aspect ratios used for figure 7 is shown in figure 8*A*, and the fractional error for the predicted V_s is 0.09 ± 0.10. The predicted S-wave velocity obtained by using BGTL with the same parameter used in figure 7 is shown in figure 8*B*. The fractional error of the predicted V_s using BGTL is

–0.02 ± 0.05. Clearly BGTL predicts V_s more accurately than KTT–GM for unconsolidated sediments at the Alpine–1 well. The predicted values indicated by red dots in figure 7 will be discussed later to demonstrate the nonuniqueness of the pore aspect ratio.

Pore Aspect Ratios

In order to predict elastic velocities using KTT, two pore aspect ratios—one for pores associated with sand grains (α_s) and the other for pores associated with clay (α_c)—are used. Xu and White (1996) suggested that α_s is close to 0.12 and α_c is close to 0.03. However, they also indicated that a single aspect ratio can closely simulate the elastic response of a uniform distribution of pores. Moreover, Pratson and others (2003) indicated that using $\alpha_c > \alpha_s$ (for example, $\alpha_c = 0.12$ and $\alpha_s = 0.06$) performed better than using $\alpha_c < \alpha_s$ in predicting
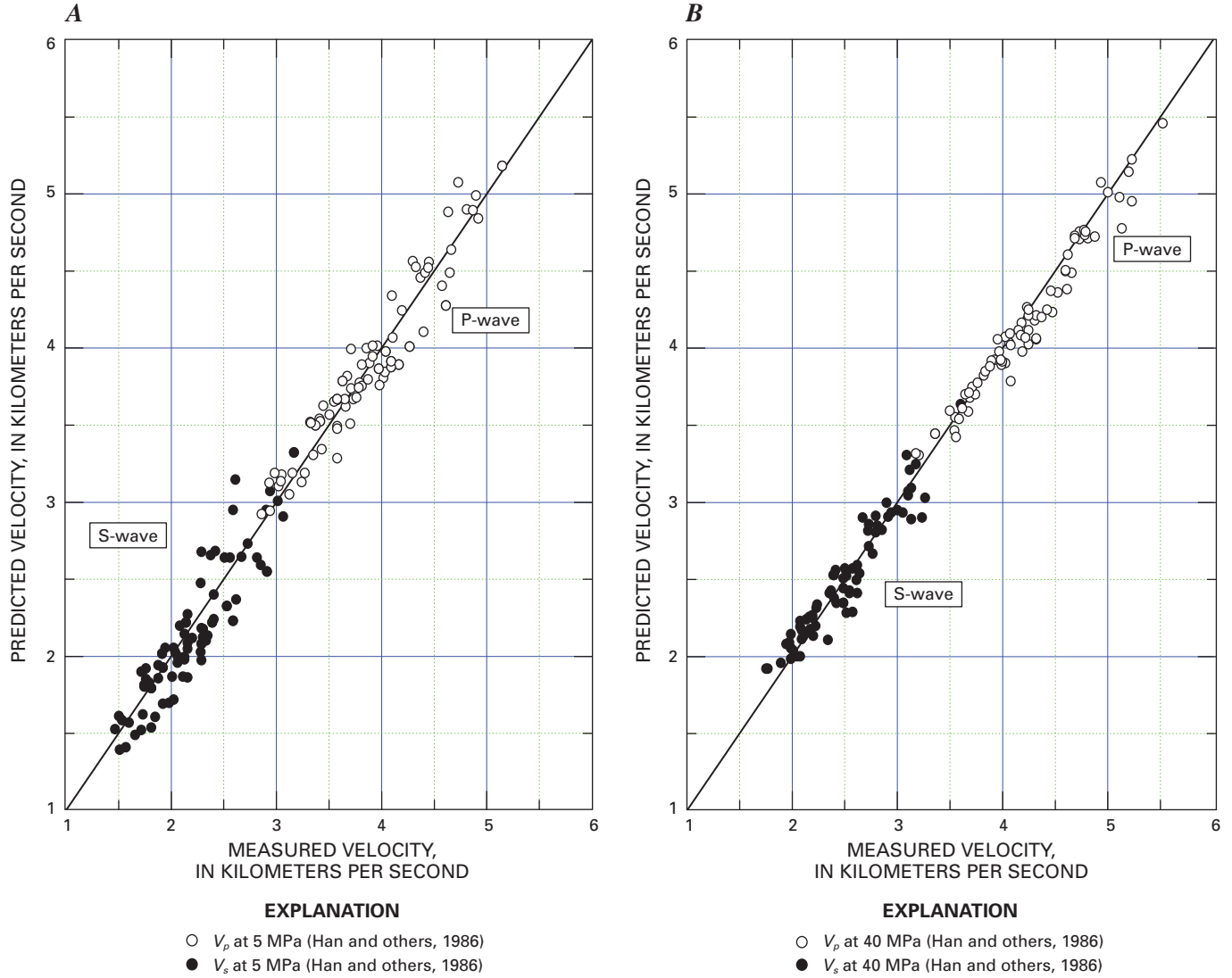
A

B

Figure 6.   Measured P- and S-wave velocities (V_p, V_s) compared with predicted velocities obtained by using the modified Biot-Gassmann theory by Lee (2002) (BGTL) for consolidated sandstones measured by Han and others (1986). *A*, Velocities measured at 5 megapascals (MPa) effective pressure compared with predicted velocities using $n = 0.73$; *B*, Velocities measured at 40 MPa effective pressure compared with predicted velocities using $n = 0.2$.

P-wave velocities from clay content using well logs acquired at the Amazon Fan during Ocean Drilling Program Leg 155. Pore aspect ratios chosen by Pratson and others (2003) appear to be opposite to the general behavior of pore aspect ratios.

   Cheng and Toksöz (1979) used KTT in order to estimate pore aspect ratios from velocities measured at various effective pressures using a linear inversion method. The inversion result of pore aspect ratios for Navajo Sandstone agrees well with ratios estimated from scanning electromagnetic micrographs. This agreement indicates that the pore aspect ratios used in KTT have physical meaning. However, Keys and Xu (2002) demonstrated that the bulk and shear modulus of dry rock can be approximated by the following formulas if the dry-rock Poisson's ratio is constant, which is approximately true with respect to porosity (Pickett, 1963; Krief and others, 1990):

$$k_d = k_{ma}(1 - \phi)^p \tag{16a}$$

$$\mu_d = \mu_{ma}(1 - \phi)^q \tag{16b}$$

where

$$p = \frac{1}{3}\sum_{l=s,c} \phi_l T_{iijj}(\alpha_l) \text{ and } q = \frac{1}{5}\sum_{l=s,c} \phi_l F(\alpha_l) \tag{17}$$

Because different combinations of pore aspect ratios and concentrations approximately satisfy equations 16a and 16b, pore aspect ratios cannot be determined uniquely. Figure 7 illustrates the non-uniqueness of pore aspect ratios. Solid lines represent modeled velocities using KTT–GM with $\alpha_s = 0.09$ and $\alpha_c = 0.045$, and red dots represent modeled velocities with $\alpha_s = 0.085$ and $\alpha_c = 0.085$. The two predicted velocities are virtually identical in spite of using different pore aspect ratios.
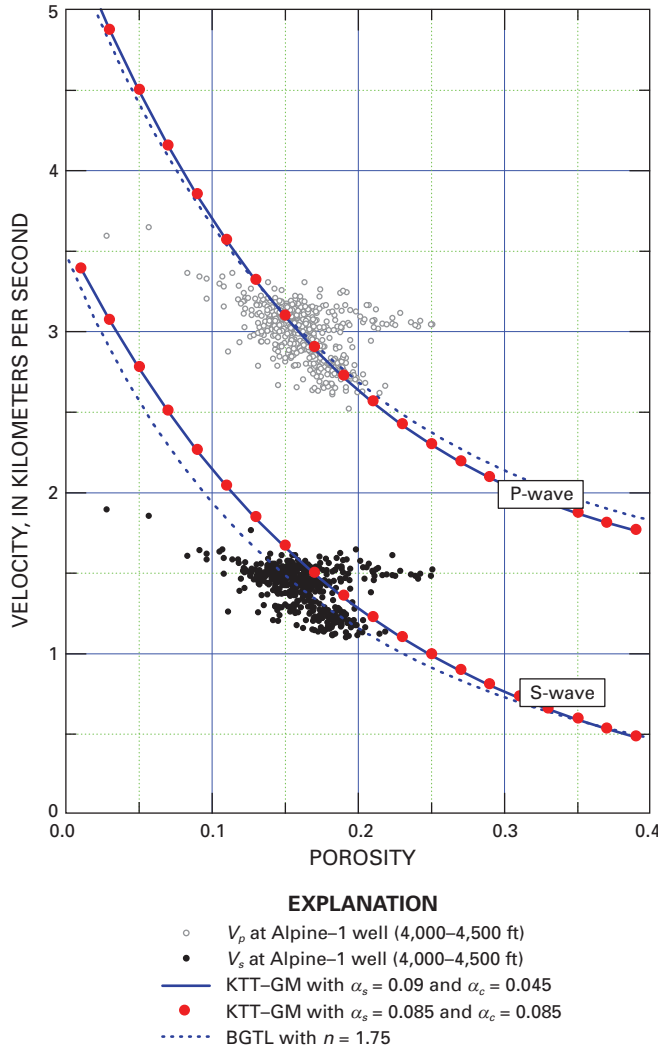
Figure 7. Well log P- and S-wave velocities (V_p, V_s) compared with predicted velocities obtained by using the modified Biot-Gassmann theory by Lee (2002) (BGTL) with $n = 1.75$ and $C_v = 0.07$ and the Kuster and Toksöz theory with Gassmann theory (KTT–GM) with $\alpha_s = 0.09$, $\alpha_c = 0.045$, and $C_v = 0.07$ for unconsolidated sediment at the Alpine–1 well, North Slope of Alaska. Dots show predicted velocities obtained by using KTT–GM with $\alpha_s = 0.085$, $\alpha_c = 0.085$, and $C_v = 0.07$. ϕ, porosity.

As shown in the previous sections, pore aspect ratios also depend on effective pressure and the degree of consolidation. Modeling results indicate that as the degree of consolidation (fig. 1) and effective pressure (fig. 4) increase, KTT requires larger pore aspect ratios. Cement that fills small gaps tends to increase the pore aspect ratio and increase velocities. Unconsolidated sediment, which contains a large number of unclosed small gaps between grain boundaries, is likely to be dominated by small aspect ratios (Xu and White, 1996). As effective pressure increases, small-aspect-ratio pores will be closed. Only the larger-aspect-ratio pores will remain, meaning that the overall pore aspect ratio of sediments increases with increasing effective pressure.

The analysis of Xu and White (1996), Pratson and others (2003), and Keys and Xu (2002), coupled with the analysis of this study, indicate that the pore aspect ratios may be considered, in practical applications, as convenient free parameters to fit the measurements, even though they are built on a firm theoretical foundation and have physical meaning.

Parameters of Modified Biot-Gassmann Theory and Pore Aspect Ratio of Kuster-Toksöz Theory

The pore aspect ratio of shaly sand is generally smaller than that of clean sand (Xu and White, 1996). Thus, according to KTT, the velocities in shaly sand are less than those in clean sand. In BGTL formulation, the parameter G partially accounts for the effect of clay on the elastic velocities, and the reduction of velocity in shaly sand increases as the clay content increases. However, as discussed below, velocities are more affected by porosity changes with respect to effective pressure for a given pore aspect ratio, which is related to BGTL parameter n.

Equation 6 indicates that as effective pressure and the degree of consolidation increase, n decreases. Thus velocities increase. Likewise, KTT indicates that as effective pressure and the degree of consolidation increase, α increases and velocities increase. Increasing n in BGTL corresponds to decreasing α in KTT, meaning the behavior of n^{-1} is similar to that of pore aspect ratio.

As shown in equations 6a and 6b, n is related to m, which is a function of porosity reduction with respect to effective pressure ($\partial\phi / \partial p$). As $\partial\phi / \partial p$ increases, m decreases and n increases. Thus, a larger $\partial\phi / \partial p$ predicts lower velocities at a given porosity and effective pressure. The same characteristic is predicted from KTT. In KTT, $\partial\phi / \partial p$ increases as the pore aspect ratio decreases and can be calculated based on equations from Toksöz and others (1976) as follows:

$$\frac{d\phi}{\phi} = \frac{-p}{k_\alpha^*} \frac{1}{E_1 - E_2 E_3 /(E_3 + E_4)} \equiv -\lambda p \qquad (18)$$

where

$$E_1 = \frac{6\mu_{ma} I}{2\pi(3k_{ma} + 4\mu_{ma})},$$

$$E_2 = \frac{6\mu_{ma}(3I - 4\pi)}{4\pi(3k_{ma} + 4\mu_{ma})},$$

$$E_3 = \frac{\alpha^2(3\_9I/4\pi)(6k_{ma} + 2\mu_{ma})}{2(1 - \alpha^2)(3k_{ma} + 4\mu_{ma})} + \frac{6\mu_{ma} I}{8\pi(3k_{ma} + 4\mu_{ma})},$$

$$E_4 = \frac{1}{2}\left[\frac{(3 - 9I/4\pi)(6k_{ma} + 2\mu_{ma})}{2(1 - \alpha^2)(3k_{ma} + 4\mu_{ma})} - \frac{3\mu_{ma}(1 - I/\pi)}{(3k_{ma} + 4\mu_{ma})} \right],$$

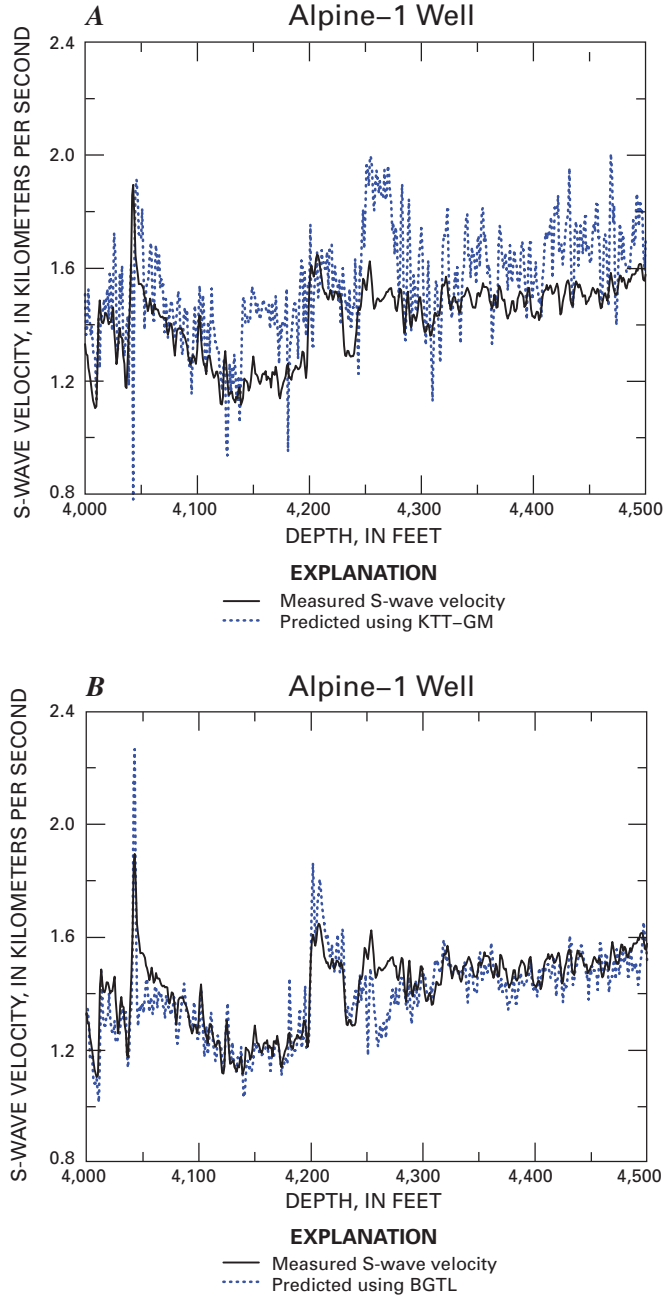$$I = \frac{2\pi\alpha}{(1 - \alpha^2)^{3/2}}\left[\cos^{-1}\alpha - \alpha(1 - \alpha^2)^{1/2} \right].$$

Figure 8. Predicted S-wave velocities compared with well log velocities at the Alpine–1 well, North Slope of Alaska. *A,* Using Kuster and Toksöz theory with Gassmann theory (KTT–GM) with $\alpha_s = 0.09$, $\alpha_c = 0.045$, and $C_v = 0.07$; *B,* Using modified Biot-Gassmann theory by Lee (2002) (BGTL) with $n = 1.75$ and $C_v = 0.07$.

The term k_a^* is the static bulk modulus of dry rock, but because of the lack of such data it is generally taken to be the dynamic bulk modulus of the dry rock (Cheng and Toksöz, 1979), which is k_d in equation 9. By assuming that the porosity change is small during the unloading, porosity with respect to effective pressure can be written as follows:

$$\phi \approx \phi_o\left(1 + \frac{d\phi}{\phi}\right) = \phi_o(1 - \lambda p), \tag{19}$$

where

ϕ_o is the initial porosity at $p = 0$.

For BGTL, equation 6b yields the following equation for porosity:

$$\phi = \frac{p}{5212}\ln\left(\frac{m-1}{4.95}\right) + \phi_o. \tag{20}$$

This form is identical to that derived from KTT, and porosity decreases linearly with effective pressure. However, the relation shown in equation 20 differs from the porosity reduction owing to compaction, which is inversely proportional to effective pressure.

Figure 9 shows the measured porosity with respect to effective pressure along with predicted porosity obtained by using equations 18 and 19 with various pore aspect ratios.
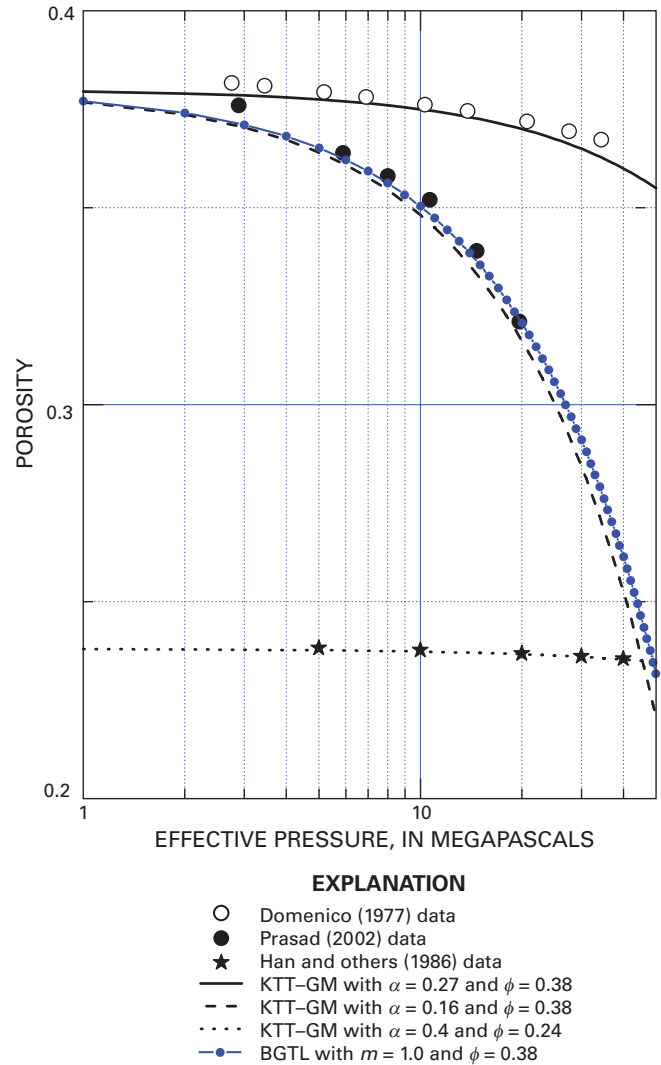

EXPLANATION

○   Domenico (1977) data
●   Prasad (2002) data
★   Han and others (1986) data
—   KTT–GM with $\alpha = 0.27$ and $\phi = 0.38$
– –   KTT–GM with $\alpha = 0.16$ and $\phi = 0.38$
· · · ·   KTT–GM with $\alpha = 0.4$ and $\phi = 0.24$
–●–   BGTL with $m = 1.0$ and $\phi = 0.38$

Figure 9. Porosity reduction with respect to effective pressure for measured data by Domenico (1977), Han and others (1986), and Prasad (2002) compared with porosity reduction predicted by Kuster and Toksöz theory with Gassmann Theory (KTT–GM) with various pore aspect ratios and by modified Biot-Gassmann theory by Lee (2002) (BGTL) with $m = 1$. ϕ, porosity.

For comparison, the result from equation 20 with $m = 1$ is also shown. Figure 9 indicates that Han and others (1986) using $\alpha = 0.4$, Domenico (1977) using $\alpha = 0.27$, and Prasad (2002) using $\alpha = 0.16$ all agree with predicted porosities. Lee (2003) indicated that $m = 5$, 1.5, and 1.0 are appropriate for Han and others (1986), Domenico (1977), and Prasad (2002) data, respectively. Figure 9 shows that $\partial\phi / \partial p$ increases as α (also m) decreases (calculated values for $m = 5$ and 1.5 (not shown in fig. 9) are almost identical to those calculated using $\alpha = 0.4$ and $\alpha = 0.27$, respectively).

As effective pressure is applied, the spheroidal pores deform and become thinner, and thin cracks are closed. However, spherical pores retain their shape but decrease in volume (Toksöz and others, 1976). Therefore, as effective pressure increases, porosity decreases and overall pore aspect ratio of sediments increases. This relation suggests that as pressure increases, the rate of porosity reduction with respect to effective pressure will be nonlinear, as opposed to the prediction by equations 18 and 20. The excellent agreement of KTT theory using a constant pore aspect ratio with observed porosity-pressure relation implies that the pore shapes do not change appreciably with pressure for data shown in figure 9. Therefore, the linear approximation of equation 20 would be valid within a limited range of effective pressure and pore shape.

Conclusions

This paper compares the performance of KTT and BGTL in predicting elastic velocities of consolidated and unconsolidated sandstones, and the following conclusions can be drawn:

1. For dry rock, KTT predicts that V_p/V_s depends on porosity as well as the pore aspect ratio, whereas BGTL predicts that V_p/V_s is independent of porosity (as does BGT) and depends on the parameter G, which is related to the clay content in the sediment.

2. For velocities in water-saturated unconsolidated sediments with high porosity, KTT–GM works better than KTT, particularly for P-wave velocity.

3. For consolidated sediments, velocities predicted by KTT–GM are similar to those predicted by BGTL. However, BGTL predicts slightly more accurate velocities for data by Han and others (1986).

4. Qualitatively, the relation of pore aspect ratios with respect to sand and clay, effective pressure, and the degree of consolidation in KTT–GM are well established. However, in practical applications, pore aspect ratios can be considered as convenient free parameters to fit the observation, because pore aspect ratios are not uniquely determined. The role of pore aspect ratios in KTT–GM is similar to the role of G and n in BGTL.

5. For unconsolidated sediments at the Alpine–1 well, North Slope of Alaska, BGTL predicts more accurate S-wave velocities from the P-wave velocity and porosity than does KTT–GM. Generally, KTT–GM overestimates the S-wave velocity for a given porosity and P-wave velocity, and the overestimation decreases as effective pressure increases.

6. Theoretically, KTT is more appropriate for predicting velocities of sediments having both thin cracks and spherical pores and for analyzing the pore shapes, but the BGTL works better for predicting velocities of sediments having spherical pores.

References Cited

Biot, M.A., 1956, Theory of propagation of elastic waves in a fluid saturated porous solid. I. Low frequency range; II. High-frequency range: Journal of Acoustical Society of America, v. 28, p. 168–191.

Blangy, J.P., Strandenes, S., Moos, D., and Nur, A., 1993, Ultrasonic velocities in sands—Revisited: Geophysics, v. 58, p. 344–356.

Carmichael, R.S., 1989, Practical handbook of physical properties of rocks and minerals, Section VI: Boca Raton, Fla., CRC Press, 741 p.

Castagna, J.P., Batzle, M.L., and Eastwood, R.L., 1985, Relationships between compressional-wave and shear-wave velocities in clastic silicate rocks: Geophysics, v. 50, p. 571–581.

Cheng, C.H., and Toksöz, M.N., 1979, Inversion of seismic velocities for the pore aspect ratio spectrum of a rock: Journal of Geophysical Research, v. 84, p. 7533–7543.

Cleary, M.P., Chen, I.W., and Lee, S.M., 1980, Self-consistent technique for predicting properties of heterogeneous materials: Journal of Engineering Mechanics, v. 106, p. 861–887.

Domenico, S.N., 1977, Elastic properties of unconsolidated porous sand reservoirs: Geophysics, v. 42, p. 1339–1368.

Gassmann, F., 1951, Elasticity of porous media: Vierteljahrsschr der Naturforschenden Gesselschaft, v. 96, p. 1–23.

Geertsma, J., and Smit, J.C., 1961, Some aspects of elastic wave propagation in fluid-saturated porous solids: Geophysics, v. 26, p. 169–181.

Hamilton, E.L., 1971, Elastic properties of marine sediments: Journal of Geophysical Research, v. 76, p. 579–604.

Han, D.H., Nur, A., and Morgan, D., 1986, Effects of porosity and clay content on wave velocities in sandstone: Geophysics, v. 51, p. 2093–2107.

Helgerud, M.B., Dvorkin, J., Nur, A., Sakai, A., and Collett, T., 1999, Elastic-wave velocity in marine sediments with gas hydrates—Effective medium modeling: Geophysical Research Letters, v. 26, p. 2021–2024.

Jakobsen, M., Hudson, J.A., Minshull, T.A., and Singh, S.C., 2000, Elastic properties of hydrate-bearing sediments using effective medium theory: Journal of Geophysical Research, v. 105, p. 561–577.

Keys, R.G., and Xu, S., 2002, An approximation for the Xu-White velocity model: Geophysics, v. 67, p. 1406–1414.

Krief, M., Garta, J., Stellingwerff, J., and Ventre, J., 1990, A petrophysical interpretation using the velocities of P and S waves (full-waveform sonic): The Log Analyst, v. 31, p. 355–369.

Kuster, G.T., and Toksöz, M.N., 1974, Velocity and attenuation of seismic waves in two-phase media. Part I. Theoretical formulations: Geophysics, v. 39, p. 587–606.

Lee, M.W., 2002, Biot-Gassmann theory for velocities of gas hydrate-bearing sediments: Geophysics, v. 67, p. 1711–1719.

Lee, M.W., 2003, Elastic properties of overpressured and unconsolidated sediments: U.S. Geological Survey Bulletin 2214, 10 p.

Lee, M.W., 2005, Well log analysis to assist the interpretation of 3-D seismic data at Milne Point, North Slope of Alaska: U.S. Geological Survey Scientific Investigations Report 2005–5048, 18 p.

Mavko, Gary, Mukerji, Tapan, and Dvorkin, Jack, 1998, The rock physics handbook—Tools for seismic analysis in porous media: Cambridge, U.K., Cambridge University Press, 329 p.

Nur, Amos, Mavko, G., Dvorkin, J., and Galmudi, D., 1998, Critical porosity, A key to relating physical properties to porosity in rocks: The Leading Edge, v. 17, p. 357–362.

Pickett, G.R., 1963, Acoustic character logs and their applications in formation evaluation: Journal of Petroleum Technology, v. 15, p. 650–667.

Prasad, Manika, 2002, Acoustic measurements in unconsolidated sands at low effective pressure and overpressure detection: Geophysics, v. 67, p. 405–412.

Pratson, L.F., Stroujkova, A., Herrick, D., Boadu, F., and Malin, P., 2003, Predicting seismic velocity and other rock properties from clay content only: Geophysics, v. 68, p. 1847–1856

Raymer, L.L., Hunt, E.R., and Gardner, J.S., 1980, An improved sonic transit time to porosity transform: SPWLA Logging Symposium, 21st annual, Transactions, paper P, 12 p.

Thomsen, Leon, 1985, Biot-consistent elastic moduli of porous rock—Low-frequency limit: Geophysics, v. 50, p. 2797–2807.

Timur, A., 1968, Velocity of compressional waves in porous media at permafrost temperatures: Geophysics, v. 33, p. 584–595.

Toksöz, M.N., Cheng, C.H., and Timur, A., 1976, Velocities of seismic waves in porous rocks: Geophysics, v. 41, p. 621–645.

Wyllie, M.R.J., Gregory, A.R., and Gardner, L.W., 1956, Elastic wave velocities in heterogeneous and porous media: Geophysics, v. 21, p. 41–70.

Xu, Shiyu, and White, R.E., 1996, A physical model for shear wave velocity prediction: Geophysical Prospecting, v. 44, p. 487–717.